

Electromagnetic form factor of pion in the field theory inspired approach.

N. N. Achasov*

Laboratory of Theoretical Physics, S. L. Sobolev Institute for Mathematics, 630090, Novosibirsk, Russian Federation

A. A. Kozhevnikov†

*Laboratory of Theoretical Physics, S. L. Sobolev Institute for Mathematics,
and Novosibirsk State University, 630090, Novosibirsk, Russian Federation*

(Dated: February 17, 2022)

A new expression for the pion form factor F_π is proposed. It takes into account the pseudoscalar meson loops and the mixing of $\rho(770)$ with heavier $\rho(1450)$ and $\rho(1700)$ resonances. The expression has correct analytical properties and can be used in both timelike and spacelike kinematical regions. The comparison is made with the existing experimental data on F_π collected with the detectors SND, CMD-2, KLOE, and the BaBar restricted to energies below 1 GeV. A good description of all four data sets is obtained. In the spacelike region, upon substituting the resonance parameters found in the timelike one, one obtains F_π in agreement with the measurements of NA7 Collaboration.

PACS numbers: 13.40.Gp, 12.40.Vv, 13.66.Bc, 14.40.Be

I. INTRODUCTION

The pion form factor F_π is an important characteristics of the low energy phenomena in particle physics related with the hadronic properties of the electromagnetic current in the theoretical scheme of the vector dominance model [1–4]. There are a number of expressions for this quantity used in the analysis of experimental data. The simplest approximate vector dominance model expression based on the effective $\gamma - \rho$ coupling $\propto \rho_\mu A_\mu$ [3],

$$F_\pi(s) = \frac{m_\rho^2 g_{\rho\pi\pi}/g_\rho}{m_\rho^2 - s - i\sqrt{s}\Gamma_{\rho\pi\pi}(s)}, \quad (1.1)$$

(for notations see Sec. III) does not possess the correct analytical properties upon the continuation to the unphysical region $0 \leq s < 4m_\pi^2$ and further to the spacelike region $s \leq 0$, nor does it takes into account the mixing of the isovector ρ -like resonances. Since, phenomenologically, [5] $g_{\rho\pi\pi}/g_\rho$ is not equal to unity—to be precise,

$$\frac{g_{\rho\pi\pi}}{g_\rho} = \left(\frac{3m_\rho \Gamma_{\rho\pi\pi} \Gamma_{\rho ee}}{2\alpha^2 q_\pi^3} \right)^{1/2} \approx 1.20 \quad (1.2)$$

—the correct normalization $F_\pi(0) = 1$ is satisfied by Eq. (1.1) only approximately. Hereafter, $\alpha = 1/137$ stands for the fine structure constant. The formula of Gounaris and Sakurai [6] respects the above normalization condition and has the correct properties under analytical continuation. However, being based on some sort of effective radius approximation for the single $\rho(770)$ resonance, it is not suited for taking into account the mixing of $\rho(770)$ with heavier isovector mesons. The expression

analogous to Eq. (1.1) based on the gauge invariant $\gamma - \rho$ coupling $\propto \rho_{\mu\nu} F_{\mu\nu}$,

$$F_\pi(s) = 1 + \frac{sg_{\rho\pi\pi}/g_\rho}{m_\rho^2 - s - i\sqrt{s}\Gamma_{\rho\pi\pi}(s)}, \quad (1.3)$$

respect the correct normalization, but does not possesses correct analytical properties and breaks unitarity. The earlier expression [7, 8] for F_π takes into account the strong isovector mixing, but has the shortcoming that the above normalization condition is satisfied only approximately, within the accuracy 20%.

The applications of the Lagrangian of Kroll, Lee, and Zumino [3] to the calculations of F_π with the meson loop contributions in the field-theoretic context are given, in particular, in Refs. [9–11]. In particular, Ref. [10] contains the comparison of the theoretical F_π with the experimental data in the spacelike kinematical region. However, the authors of Ref. [10] refrained from the application of their expression in the timelike region despite the fact that the high statistics experimental data collected with the detectors SND [12] and CMD-2 [13] were available at that time.

The purpose of the present work is to obtain the expression for the pion form factor which possesses the correct analytical properties in the entire kinematic domain and takes into account the mixing of $\rho(770)$ with the heavier resonances $\rho(1450)$ and $\rho(1700)$. By restricting the consideration to the inclusion of the pseudoscalar meson loops $\pi^+\pi^-$ and $K\bar{K}$, which admits the analytical treatment and is valid at energies below 1 GeV, the new expression is found and compared with the existing data on F_π collected with the detectors SND [12] CMD-2 [13], KLOE [14], and BaBar [15].

Below, in Sec. II, the method is described by which the loop contributions to the vector–meson propagators are taken into account. The expression for the form factor $F_\pi(s)$ is given in Sec. III. Section IV is devoted to the analysis of available new experimental data on $F_\pi(s)$ [12–15]. Section V contains the discussion of the obtained

* achasov@math.nsc.ru

† kozhev@math.nsc.ru

results. The conclusions are stated in Sec. VI. The Appendix is devoted to the description of the method by which the resonance mixing is taken into account.

II. THE LOOP CONTRIBUTIONS TO THE VECTOR MESON PROPAGATOR

Let us give some details necessary for the derivation of the expression for the pion form factor. They refer to the pseudoscalar loop contributions. For the sake of brevity, the notation

$$\rho_1 \equiv \rho(770), \rho_2 \equiv \rho(1450), \rho_3 \equiv \rho(1700) \quad (2.1)$$

is used hereafter for the isovector resonances involved in the consideration.

The starting point is the effective Lagrangian describing the SU(3) invariant interaction of the vector resonances with the pair of pseudoscalar mesons [16, 17]. Restricted to the couplings of the isovector resonances ρ_i , $i = 1, 2, 3$, with the pair of pions and kaons ($P = \pi, K$), this Lagrangian looks like

$$\begin{aligned} \mathcal{L}_{\rho_i PP} = ig_{\rho_i \pi \pi} \rho_{i\mu}^0 \left\{ \frac{1}{2} [K^- \partial_\mu K^+ - K^+ \partial_\mu K^- - \right. \\ \left. \bar{K}^0 \partial_\mu K^0 + K^0 \partial_\mu \bar{K}^0] + \pi^- \partial_\mu \pi^+ - \right. \\ \left. - \pi^+ \partial_\mu \pi^- \right\}. \end{aligned} \quad (2.2)$$

The partial width of the decay $\rho_i \rightarrow P\bar{P}$ calculated from the above effective Lagrangian, is

$$\Gamma_{\rho_i \rightarrow PP}(s) = \frac{g_{\rho_i PP}^2 s^{1/2} v_P^3(s)}{48\pi}, \quad (2.3)$$

where s stands for the (virtual) mass squared of the decaying resonance ρ_i , and

$$v_P(s) = \sqrt{1 - \frac{4m_P^2}{s}} \quad (2.4)$$

is the velocity of the final meson in the rest frame of the decaying resonance. Applying the Cutkosky cutting rule to the diagram in Fig. 1 one finds that the imaginary part of the diagonal polarization operator caused by the specific real intermediate state $P\bar{P}$ is related to the corresponding partial decay width according to the expression

$$\text{Im}\Pi_{\rho_i \rho_i}^{P\bar{P}}(s) = \sqrt{s}\Gamma_{\rho_i PP}(s). \quad (2.5)$$

In the present work, the real intermediate states $\pi^+\pi^-$, K^+K^- , and $K^0\bar{K}^0$ are taken into account, hence

$$\text{Im}\Pi_{\rho_i \rho_i}(s) = \sum_{P=\pi^+, K^+, K^0} \text{Im}\Pi_{\rho_i \rho_i}^{P\bar{P}}(s).$$

The diagonal and nondiagonal polarization operators for the specific loop $P\bar{P}$ are calculated from the dispersion integral. Here the version of this integral is defined

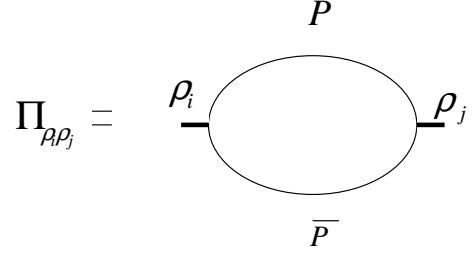


FIG. 1. The meson loop diagram contributing to both the diagonal polarization operator $\Pi_{\rho_i \rho_i}$ —resulting, in particular, in the finite width of the resonance— and the nondiagonal one $\Pi_{\rho_i \rho_j}$, responsible for the $\rho_i \rho_j$ resonance mixing; $P = \pi^+, K^+, K^0$.

which automatically provides the condition $\Pi_{\rho_i \rho_j}(0) = 0$, in agreement with the conservation of the vector current. To this end, the dispersion relation should be written for the quantity $\Pi_{\rho_i \rho_j}(s)/s$. Then, one has

$$\begin{aligned} \frac{\Pi_{\rho_i \rho_j}^{P\bar{P}}(s)}{s} = \frac{1}{\pi} \int_{4m_P^2}^{\infty} \frac{\text{Im}\Pi_{\rho_i \rho_j}^{P\bar{P}}(s') ds'}{s'(s' - s - i\varepsilon)} = \\ \frac{g_{\rho_i PP} g_{\rho_j PP}}{48\pi^2} \int_{4m_P^2}^{\infty} \frac{v_P^3(s') ds'}{s' - s - i\varepsilon}. \end{aligned} \quad (2.6)$$

One can evaluate this dispersion integral in the unphysical region $0 \leq s < 4m_P^2$, where $\text{Im}\Pi_{\rho_i \rho_j} = 0$, and no pole is encountered. But, the integral is still divergent at $s' \rightarrow \infty$. The divergence can be regularized by taking the cutoff $s'_{\text{max}} = \Lambda^2$. The integration can be fulfilled with the change of the integration variable $\sigma^2 = v_P^2(s') = 1 - 4m_P^2/s'$:

$$\begin{aligned} I(s) \equiv \int_{4m_P^2}^{\Lambda^2} \frac{ds'}{s' - s} \left(1 - \frac{4m_P^2}{s'}\right)^{3/2} = \int_0^{1-2m_P^2/\Lambda^2} d\sigma \times \\ \frac{8m_P^2 \sigma^4}{(1 - \sigma^2)(4m_P^2 - s + \sigma^2)} = -\frac{8m_P^2}{s} + \\ 2 \left(\frac{4m_P^2}{s} - 1\right)^{3/2} \arctan \frac{1}{\sqrt{\frac{4m_P^2}{s} - 1}} + 4 \ln \frac{\Lambda}{m_P}. \end{aligned}$$

The logarithmic divergence can be removed by fixing $\text{Re}I(m_V^2) = 0$. The diagonal elements $\Pi_{\rho_i \rho_i} \equiv \Pi_{\rho_i \rho_i}(s)$ can be represented in the form

$$\Pi_{\rho_i \rho_i} = \frac{sg_{\rho_i \pi \pi}^2}{48\pi^2} \left[\Pi_\pi(s, m_{\rho_i}^2) + \frac{1}{2} \Pi_K(s, m_{\rho_i}^2) \right], \quad (2.7)$$

where the factor 1/2 in the second term is due to the flavor SU(3) relation $g_{\rho_i KK} = \frac{1}{2}g_{\rho_i \pi \pi}$ [see Eq. (2.2)] and that two isotopic $K\bar{K}$ modes contribute.

The expressions for $\Pi_{\pi, K}(s, m_V^2)$ are represented in the following form. Since the pion is the lightest hadron, the function $\Pi_\pi(s, m_V^2)$ looks as

$$\begin{aligned}
\Pi_\pi(s, m_V^2) &= 8m_\pi^2 \left(\frac{1}{m_V^2} - \frac{1}{s} \right) + v_\pi^3(m_V^2) \ln \frac{1+v_\pi(m_V^2)}{1-v_\pi(m_V^2)} + v_\pi^3(s) \left[i\pi - \ln \frac{1+v_\pi(s)}{1-v_\pi(s)} \right], \text{ if } s \geq 4m_\pi^2; \\
\Pi_\pi(s, m_V^2) &= 8m_\pi^2 \left(\frac{1}{m_V^2} - \frac{1}{s} \right) + v_\pi^3(m_V^2) \ln \frac{1+v_\pi(m_V^2)}{1-v_\pi(m_V^2)} + 2\bar{v}_\pi^3(s) \arctan \frac{1}{\bar{v}_\pi(s)}, \text{ if } 0 \leq s < 4m_\pi^2; \\
\Pi_\pi(s, m_V^2) &= 8m_\pi^2 \left(\frac{1}{m_V^2} - \frac{1}{s} \right) + v_\pi^3(m_V^2) \ln \frac{1+v_\pi(m_V^2)}{1-v_\pi(m_V^2)} - v_\pi^3(s) \ln \frac{v_\pi(s)+1}{v_\pi(s)-1}, \text{ if } s < 0.
\end{aligned} \tag{2.8}$$

The function $\Pi_K(s, m_V^2)$ looks different depending on the

mass of the vector meson m_V . If $m_V > 2m_K$, as is the case for $V = \rho(1450)$ and $\rho(1700)$, the expression is

$$\begin{aligned}
\Pi_K(s, m_V^2) &= 8m_K^2 \left(\frac{1}{m_V^2} - \frac{1}{s} \right) + v_K^3(m_V^2) \ln \frac{1+v_K(m_V^2)}{1-v_K(m_V^2)} + v_K^3(s) \left[i\pi - \ln \frac{1+v_K(s)}{1-v_K(s)} \right], \text{ if } s \geq 4m_K^2; \\
\Pi_K(s, m_V^2) &= 8m_K^2 \left(\frac{1}{m_V^2} - \frac{1}{s} \right) + v_K^3(m_V^2) \ln \frac{1+v_K(m_V^2)}{1-v_K(m_V^2)} + 2\bar{v}_K^3(s) \arctan \frac{1}{\bar{v}_K(s)}, \text{ if } 0 \leq s < 4m_K^2; \\
\Pi_K(s, m_V^2) &= 8m_K^2 \left(\frac{1}{m_V^2} - \frac{1}{s} \right) + v_K^3(m_V^2) \ln \frac{1+v_K(m_V^2)}{1-v_K(m_V^2)} - v_K^3(s) \ln \frac{v_K(s)+1}{v_K(s)-1}, \text{ if } s < 0.
\end{aligned} \tag{2.9}$$

If $m_V < 2m_K$, as is the case for $V = \rho(770)$, the expres-

sion is

$$\begin{aligned}
\Pi_K(s, m_V^2) &= 8m_K^2 \left(\frac{1}{m_V^2} - \frac{1}{s} \right) - 2\bar{v}_K^3(m_V^2) \arctan \frac{1}{\bar{v}_K(m_V^2)} + v_K^3(s) \left[i\pi - \ln \frac{1+v_K(s)}{1-v_K(s)} \right], \text{ if } s \geq 4m_K^2; \\
\Pi_K(s, m_V^2) &= 8m_K^2 \left(\frac{1}{m_V^2} - \frac{1}{s} \right) - 2\bar{v}_K^3(m_V^2) \arctan \frac{1}{\bar{v}_K(m_V^2)} + 2\bar{v}_K^3(s) \arctan \frac{1}{\bar{v}_K(s)}, \text{ if } 0 \leq s < 4m_K^2; \\
\Pi_K(s, m_V^2) &= 8m_K^2 \left(\frac{1}{m_V^2} - \frac{1}{s} \right) - 2\bar{v}_K^3(m_V^2) \arctan \frac{1}{\bar{v}_K(m_V^2)} - v_K^3(s) \ln \frac{v_K(s)+1}{v_K(s)-1}, \text{ if } s < 0.
\end{aligned} \tag{2.10}$$

The function $v_P(s)$ ($P = \pi, K$) is given by Eq. (2.4), while

$$\bar{v}_P(s) = \sqrt{\frac{4m_P^2}{s}} - 1. \tag{2.11}$$

Note that the expressions Eqs. (2.8), (2.9), and (2.10) have the property that their real parts vanish at $s = m_V^2$:

$$\text{Re}\Pi_{\pi,K}(m_V^2, m_V^2) = 0.$$

III. THE EXPRESSION FOR THE PION FORM FACTOR

The new expression for the pion form factor which automatically respects the current conservation condition $F_\pi(0) = 1$ and possesses the correct analytical properties

over the entire s axis, looks like

$$\begin{aligned}
F_\pi(s) &= (g_{\gamma\rho_1}, g_{\gamma\rho_2}, g_{\gamma\rho_3}) G^{-1} \begin{pmatrix} g_{\rho_1\pi\pi} \\ g_{\rho_2\pi\pi} \\ g_{\rho_3\pi\pi} \end{pmatrix} + \\
&\frac{g_{\gamma\omega}\Pi_{\rho_1\omega}}{D_\omega\Delta} (g_{11}g_{\rho_1\pi\pi} + g_{12}g_{\rho_2\pi\pi} + \\
&g_{13}g_{\rho_3\pi\pi}).
\end{aligned} \tag{3.1}$$

The notations are as follows. The quantity

$$g_{\gamma V} = \frac{m_V^2}{g_V}, \tag{3.2}$$

($V = \rho_{1,2,3}, \omega$) is introduced in such a way that $eg_{\gamma V}$, where e is the electric charge, is the γV transition amplitude. As usual, the coupling constant g_V is calculated from the electronic width

$$\Gamma_{V \rightarrow e^+e^-} = \frac{4\pi\alpha^2 m_V}{3g_V^2} \tag{3.3}$$

of the resonance V . The matrix of inverse propagators

$$G = \begin{pmatrix} D_{\rho_1} & -\Pi_{\rho_1\rho_2} & -\Pi_{\rho_1\rho_3} \\ -\Pi_{\rho_1\rho_2} & D_{\rho_2} & -\Pi_{\rho_2\rho_3} \\ -\Pi_{\rho_1\rho_3} & -\Pi_{\rho_2\rho_3} & D_{\rho_3} \end{pmatrix} \quad (3.4)$$

is responsible for the $\rho(770)$ - $\rho(1450)$ - $\rho(1700)$ mixing [7, 8, 18–20], and $\Delta = \det G$. See the Appendix for more detail. The inverse propagators of the ρ_i -resonance ($i = 1, 2, 3$) are

$$D_{\rho_i} = m_{\rho_i}^2 - s - \Pi_{\rho_i\rho_i}, \quad (3.5)$$

where the diagonal polarization operator $\Pi_{\rho_i\rho_i}$ can be expressed through the functions $\Pi_\pi(s, m_V^2)$ and $\Pi_K(s, m_V^2)$ described in Sec. II. The nondiagonal polarization operators are the following:

$$\begin{aligned} \Pi_{\rho_1\rho_2} &= \frac{g_{\rho_2\pi\pi}}{g_{\rho_1\pi\pi}} \Pi_{\rho_1\rho_1}, \\ \Pi_{\rho_1\rho_3} &= \frac{g_{\rho_3\pi\pi}}{g_{\rho_1\pi\pi}} \Pi_{\rho_1\rho_1}, \\ \Pi_{\rho_2\rho_3} &= \frac{g_{\rho_2\pi\pi}g_{\rho_3\pi\pi}}{g_{\rho_1\pi\pi}^2} \Pi_{\rho_1\rho_1} + sa_{23}. \end{aligned} \quad (3.6)$$

The quantity a_{23} is the dimensionless phenomenological free parameter. No such parameter is introduced in $\Pi_{\rho_1\rho_2}$ and $\Pi_{\rho_1\rho_3}$ because it would result in a shift of the $\rho(770)$ resonance peak position. See the Appendix and Refs. [7, 8].

The term $\propto \Pi_{\rho_1\omega}$ in Eq. (3.1) takes into account the $\rho(770) - \omega(782)$ mixing. The basic quantities in this contribution are the following. The inverse propagator of the meson $\omega(782)$ is taken in the form

$$D_\omega = m_\omega^2 - s - i\sqrt{s}\Gamma_\omega, \quad (3.7)$$

where the energy-dependent width

$$\Gamma_\omega \equiv \Gamma_\omega(s) = \Gamma_{\omega 3\pi}(s) + \Gamma_{\omega\pi\gamma}(s) + \Gamma_{\omega\eta\gamma}(s)$$

includes the dominant decay mode $\omega(782) \rightarrow \pi^+\pi^-\pi^0$ and the radiative ones. The tree pion decay width is represented in the form

$$\Gamma_{\omega 3\pi}(s) = \frac{g_{\omega\rho_1\pi}^2}{4\pi} W_{3\pi}(s),$$

where $W_{3\pi}(s)$ is the phase space volume of the final $\pi^+\pi^-\pi^0$ state:

$$\begin{aligned} W_{3\pi}(s) &= \int_{2m_\pi}^{\sqrt{s}-m_\pi} dm m^2 \Gamma_{\rho_1\pi\pi}(m^2) q_{\rho\pi}^3 \int_{-1}^1 dx \times \\ &\quad (1-x^2) \left| \frac{1}{D_{\rho_1}(m^2)} + \frac{1}{D_{\rho_1}(m_+^2)} + \right. \\ &\quad \left. \frac{1}{D_{\rho_1}(m_-^2)} \right|^2. \end{aligned} \quad (3.8)$$

Here, m is the invariant mass of the $\pi^+\pi^-$ pair while m_\pm refers to the $\pi^\pm\pi^0$ one:

$$\begin{aligned} m_\pm^2 &= \frac{1}{2}(s + 3m_\pi^2 - m^2) \pm \\ &\quad xq_{\rho\pi} \sqrt{s \left(1 - \frac{4m_\pi^2}{m^2} \right)}, \end{aligned} \quad (3.9)$$

and $q_{\rho\pi} = q(\sqrt{s}, m, m_\pi)$. Here and in what follows,

$$\begin{aligned} q(\sqrt{s}, m_a, m_b) &= \frac{1}{2\sqrt{s}} \{ [s - (m_a + m_b)^2] \times \\ &\quad [s - (m_a - m_b)^2] \}^{1/2} \end{aligned} \quad (3.10)$$

is the momentum of the particles a or b with the masses m_a or m_b , respectively, in the rest reference frame of the decaying particle whose invariant mass is \sqrt{s} . The coupling constant $g_{\omega\rho\pi}$ is evaluated from the $\omega \rightarrow \pi^+\pi^-\pi^0$ decay width. The energy-dependent radiative width $\Gamma_{VP\gamma}(s)$, where $V = \rho_1, \omega$, $P = \pi, \eta$, is related to the radiative width on the mass shell $\Gamma_{VP\gamma}^{(0)} \equiv \Gamma_{VP\gamma}(m_V^2)$ in accord with the relation

$$\Gamma_{VP\gamma}(s) = \Gamma_{VP\gamma}^{(0)} \frac{q_P^3(s)}{q_P^3(m_V^2)}, \quad (3.11)$$

and $q_P(s) = q(\sqrt{s}, m_P, 0)$ is the momentum of the pseudoscalar meson P in the rest frame of the decaying vector meson V . The quantity

$$\Pi_{\rho_1\omega} = \frac{s}{m_\omega^2} \Pi'_{\rho_1\omega} + i\sqrt{s}\Gamma_{\omega\pi\gamma}(s)\Gamma_{\rho\pi\gamma}(s) \quad (3.12)$$

is the polarization operator of the $\rho(770) - \omega(782)$ mixing. The real part $s\Pi'_{\rho_1\omega}/m_\omega^2$ is chosen in such a way that it vanishes at $s = 0$, and $\Pi'_{\rho_1\omega}$ is a free parameter. The contributions to $\text{Im}\Pi_{\rho_1\omega}$ from the $\eta\gamma$ intermediate state can be neglected in comparison with the $\pi\gamma$ one. If not fitted, the masses and partial widths of particles and resonances involved in the treatment are taken from the Review of Particle Physics [5].

Note that the isovector-isoscalar type of weak mixing is essential only for the $\rho(770) - \omega(782)$ system because it is enhanced due to the small mass difference of these resonances. As for other isovector-isoscalar mixings $\rho(1450) - \omega(782)$ and $\rho(1700) - \omega(782)$, there is no enhancement due to the mass proximity, and one can neglect $\Pi_{\rho_2,3\omega}$ in what follows. The coupling constant of the direct transition $\omega \rightarrow \pi^+\pi^-$ is neglected, too. The reason for this is explained in the Appendix. See Eq. (A8) and the discussion around it. The quantities g_{11} , g_{12} , g_{13} are, respectively,

$$\begin{aligned} g_{11} &= D_{\rho_2}D_{\rho_3} - \Pi_{\rho_2\rho_3}^2, \\ g_{12} &= D_{\rho_3}\Pi_{\rho_1\rho_2} + \Pi_{\rho_1\rho_3}\Pi_{\rho_2\rho_3}, \\ g_{13} &= D_{\rho_2}\Pi_{\rho_1\rho_3} + \Pi_{\rho_1\rho_2}\Pi_{\rho_2\rho_3}. \end{aligned}$$

See Eq. (A5) in the Appendix.

When checking the form factor normalization $F_\pi(0) = 1$, one should have in mind that the $\rho\omega$ mixing is negligible at $s = 0$, because, at this energy squared, there is no

enhancement of the effect due to the proximity of m_ω and m_ρ . The same is true for other contributions violating G-parity conservation. Neglecting the above contributions results in the correct normalization $F_\pi(0) = 1$, if one takes

$$\frac{g_{\rho_1\pi\pi}}{g_{\rho_1}} + \frac{g_{\rho_2\pi\pi}}{g_{\rho_2}} + \frac{g_{\rho_3\pi\pi}}{g_{\rho_3}} = 1. \quad (3.13)$$

Indeed, the mixings due to strong interactions $\Pi_{\rho_i\rho_j}$ vanish at $s = 0$, and $F_\pi(0)$ reduces to the above sum. This is the reason for the s in front of a_{23} in Eq. (3.6). The comparison of the new expression Eq. (3.1) with the latest experimental data [12–15] obtained in e^+e^- annihilation is presented in the next section.

IV. THE DATA ANALYSIS AND RESULTS

The experimental data on the reaction $e^+e^- \rightarrow \pi^+\pi^-$ collected by the collaborations SND [12], CMD-2 [13], KLOE [14], and BaBar [15] are chosen for the analysis in the framework of the field-theory-inspired approach to the pion form factor presented in this work. As for the BaBar data set, we restrict ourselves by the points with

$\sqrt{s} \leq 1$ GeV, because, at the first stage of the study, the proposed expression for the polarization operator is restricted to include only $\pi^+\pi^-$ and $K\bar{K}$ loops.

The original $e^+e^- \rightarrow \pi^+\pi^-$ data of the SND, CMD-2, and KLOE Collaborations are presented in two distinct forms. The first one is the form factor with the vacuum polarization effect included. The BaBar Collaboration does not present their results in this form. The second form is the so-called bare cross section. This quantity is undressed from the vacuum polarization effects, but includes the final state radiation. All four groups present their data in this form. For the purpose of uniformity of presentation, the analysis of the present work refers to the bare cross section

$$\sigma_{\text{bare}} = \frac{8\pi\alpha^2}{3s^{5/2}} |F_\pi(s)|^2 q_\pi^3(s) \left[1 + \frac{\alpha}{\pi} a(s) \right], \quad (4.1)$$

where $F_\pi(s)$ is given by Eq. (3.1),

$$q_\pi(s) = \sqrt{s} v_\pi(s)/2$$

is the momentum of the final pion, and the function $a(s)$ allows for the radiation of a photon by the final pions. In the case of the pointlike pions, it has the form [12, 22–25]

$$\begin{aligned} a(s) = & \frac{1+v_\pi^2}{v_\pi} \left[4\text{Li}_2\left(\frac{1-v_\pi}{1+v_\pi}\right) + 2\text{Li}_2\left(-\frac{1-v_\pi}{1+v_\pi}\right) - 3\ln\frac{2}{1+v_\pi} \ln\frac{1+v_\pi}{1-v_\pi} - 2\ln v_\pi \ln\frac{1+v_\pi}{1-v_\pi} \right] - \\ & 3\ln\frac{4}{1-v_\pi^2} - 4\ln v_\pi + \frac{1}{v_\pi^3} \left[\frac{5}{4}(1+v_\pi^2)^2 - 2 \right] \ln\frac{1+v_\pi}{1-v_\pi} + \frac{3(1+v_\pi^2)}{2v_\pi^2}. \end{aligned} \quad (4.2)$$

Here, $v_\pi \equiv v_\pi(s)$ is given by Eq. (2.4), and

$$\text{Li}_2(x) = - \int_0^x dt \frac{\ln(1-t)}{t}.$$

First of all, no fit with the single $\rho(770)$ resonance contribution, based on Eq. (3.1) in which both $g_{\rho_2\pi\pi}$ and $g_{\rho_3\pi\pi}$ are set to zero, is capable of satisfactory description of all four data sets, even with the $\rho\omega$ mixing effect being taken into account. Although the formula with the single resonance works well in the $\rho\omega$ resonance region, the curve at the far-right shoulder of the $\rho(770)$ resonance peak does not follow the data points.

Taking into account the resonance ρ_2 , but with the neglect of the ρ_3 one, results in a rather poor fit, too. This is because the normalization condition $F_\pi(0) = 1$ reduces, in this case, to the rather restrictive sum rule

$$\frac{g_{\rho_1\pi\pi}}{g_{\rho_1}} + \frac{g_{\rho_2\pi\pi}}{g_{\rho_2}} = 1,$$

which fixes completely the ρ_2 contribution to the $e^+e^- \rightarrow \pi^+\pi^-$ reaction amplitude in a way that forbids the successful fit. Specifically, the ratio $g_{\rho_2\pi\pi}/g_{\rho_2}$ turns out to be

too small due to the fact that the universality condition $g_{\rho_1\pi\pi}/g_{\rho_1} \approx 1$ is satisfied for the couplings of $\rho(770)$. See Eq. (1.2). Hence, the ρ_2 resonance contribution turns out to be smaller than necessary for reconciling the calculations with the data. The third resonance $\rho_3 \equiv \rho(1700)$ is required in order both to preserve the approximate universality condition and to allow a freedom in the variation of the $\rho_2 \equiv \rho(1450)$ couplings.

Free parameters, which should be determined from comparison with the existing data [12–15], are the masses of the resonances $\rho(770)$ and $\omega(782)$, the coupling constants $g_{\rho_{1,2,3} \rightarrow \pi\pi}$ of the resonances $\rho_{1,2,3}$ with the $\pi^+\pi^-$ state, the coupling constants $g_{\rho_{1,2}}$ and g_ω parametrizing the $\rho_{1,2,3}$ and $\omega(782)$ leptonic decay widths [see Eq. (3.3)], and the real part of the polarization operator of the $\rho(770) - \omega(782)$ mixing $\Pi'_{\rho_1\omega}$. Note that g_{ρ_3} is not free but should be determined from the sum rule Eq. (3.13). At last, there is the parameter a_{23} [see Eq. (3.6)] that defines $\text{Re}\Pi_{\rho_2\rho_3}$. Since we restrict our analysis to the energy range below 1 GeV, the masses of the resonances $\rho(1450)$ and $\rho(1700)$ are fixed to, respectively, $m_{\rho_2} = 1.45$ GeV and $m_{\rho_3} = 1.7$ GeV.

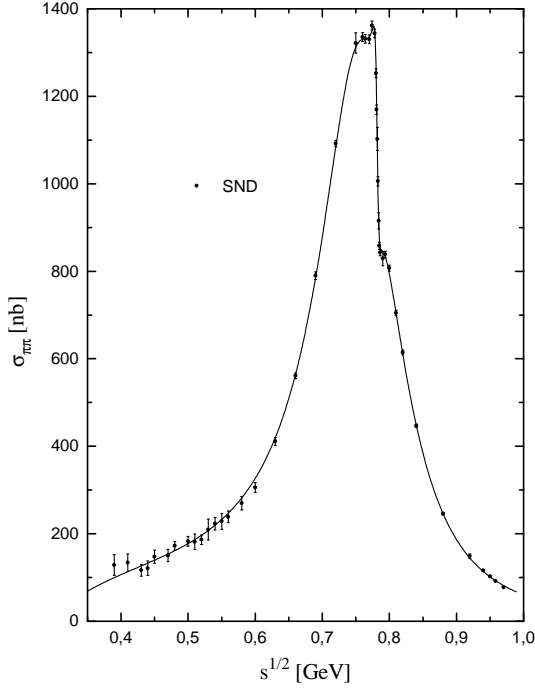


FIG. 2. The bare cross section, Eq. (4.1), calculated with the resonance parameters obtained from fitting the SND data [12] listed in Table I. Experimental points are from Ref. [12].

So, the total set of free parameters is

$$m_{\rho_1}, g_{\rho_1 \pi \pi}, g_{\rho_1}, m_{\omega}, g_{\omega}, \Pi'_{\rho_1 \omega}, g_{\rho_2 \pi \pi}, g_{\rho_2}, g_{\rho_3 \pi \pi}, a_{23}. \quad (4.3)$$

Their obtained values, found from fitting the bare cross section Eq. (4.1), side-by-side with the corresponding χ^2 per number of degrees of freedom, are listed in Table I separately for the four independent measurements of SND [12], CMD-2 [13], KLOE [14], and the BaBar data [15] restricted to the low-energy range $\sqrt{s} \leq 1$ GeV by the reason explained earlier. The bare cross section evaluated with the parameters of Table I is compared with the SND [12], CMD-2 [13], KLOE [14], and BaBar [15] data shown in Figs. 2, 3, 4, and 5, respectively.

As far as the specific values of the obtained parameters in the Table I are concerned, those corresponding to the $\rho(770) - \omega(782)$ resonance system agree satisfactorily for all four experiments [12–15]. The agreement of the coupling constants of the resonances $\rho(1450)$ and $\rho(1700)$ is poor but, taking into account the large uncertainties in their determination, is not crucial. This is justifiable, because the energy range $\sqrt{s} \leq 1$ GeV is not a proper place for extraction of the coupling constants of the above resonances. The widths of $\rho(1450)$ and $\rho(1700)$, in their respective energy ranges, are known to be saturated by the complicated final states $\rho\pi\pi$, $\omega\pi$, etc., not the $\pi^+\pi^-$ one [5]. Taking into account these decay modes is necessary at energies $\sqrt{s} > 1$ GeV. Unfortunately, taking into account the real parts of the polarization operators arising due to the mentioned complicated states is hardly

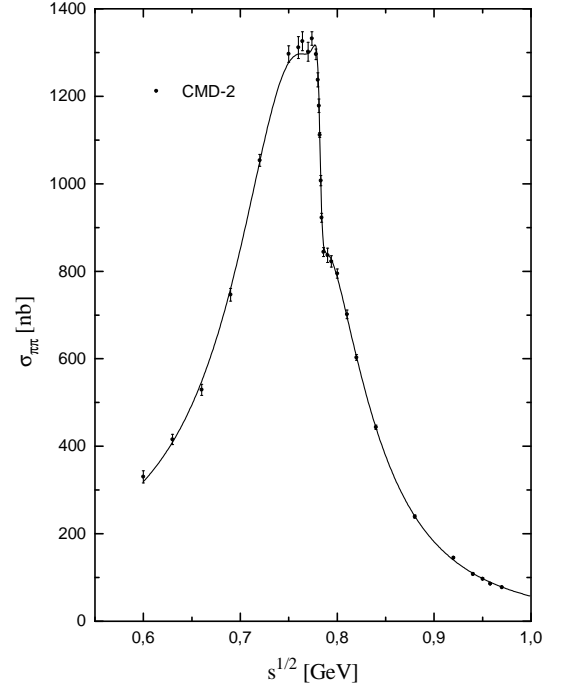


FIG. 3. The same as in Fig. 2, but evaluated with the parameters obtained from fitting the CMD-2 data [13]. Experimental points are from Ref. [13].

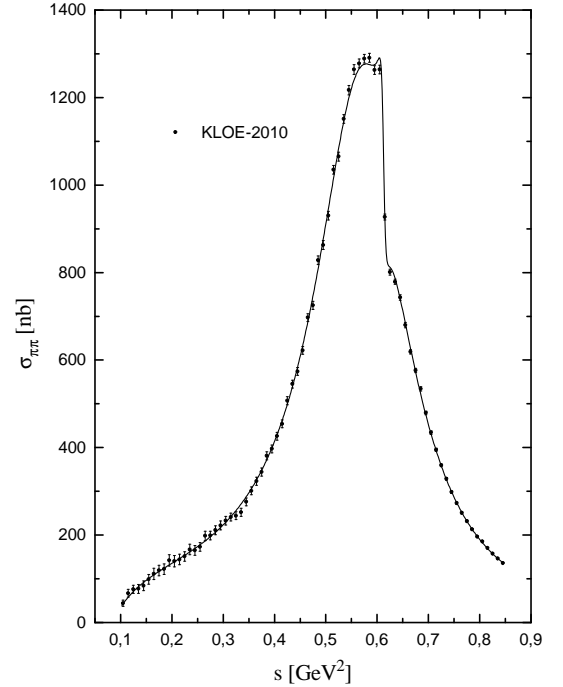


FIG. 4. The same as in Fig. 2, but evaluated with the parameters obtained from fitting the KLOE-2010 data [14]. Experimental points are from Ref. [14].

TABLE I. The resonance parameters found from fitting the data from SND [12], CMD-2 [13], KLOE10 [14], and the BaBar data [15] restricted to the energies $\sqrt{s} \leq 1$ GeV.

parameter	SND	CMD-2	KLOE10	BaBar
m_{ρ_1} [MeV]	773.76 ± 0.21	774.70 ± 0.26	774.36 ± 0.12	773.92 ± 0.10
$g_{\rho_1 \pi \pi}$	5.798 ± 0.006	5.785 ± 0.008	5.778 ± 0.006	5.785 ± 0.004
g_{ρ_1}	5.130 ± 0.004	5.193 ± 0.006	5.242 ± 0.003	5.167 ± 0.002
m_ω [MeV]	781.76 ± 0.08	782.33 ± 0.06	782.94 ± 0.11	782.04 ± 0.10
g_ω	17.13 ± 0.30	18.43 ± 0.47	18.27 ± 0.45	17.05 ± 0.29
$10^3 \Pi'_{\rho_1 \omega}$ [GeV ²]	4.00 ± 0.07	3.97 ± 0.10	3.98 ± 0.09	4.00 ± 0.06
$g_{\rho_2 \pi \pi}$	0.71 ± 0.35	0.79 ± 0.26	0.019 ± 0.004	0.21 ± 0.04
g_{ρ_2}	8.0 ± 4.4	7.6 ± 3.4	0.22 ± 0.07	4.0 ± 1.0
$g_{\rho_3 \pi \pi}$	$0.20^{+1.20}_{-0.17}$	0.76 ± 0.75	$0.055^{+0.088}_{-0.043}$	$0.011^{+0.479}_{-0.007}$
a_{23}	0.002 ± 0.011	-0.016 ± 0.057	-0.014 ± 0.040	-0.0005 ± 0.0009
$\chi^2/N_{\text{d.o.f.}}$	54/35	34/19	87/65	216/260

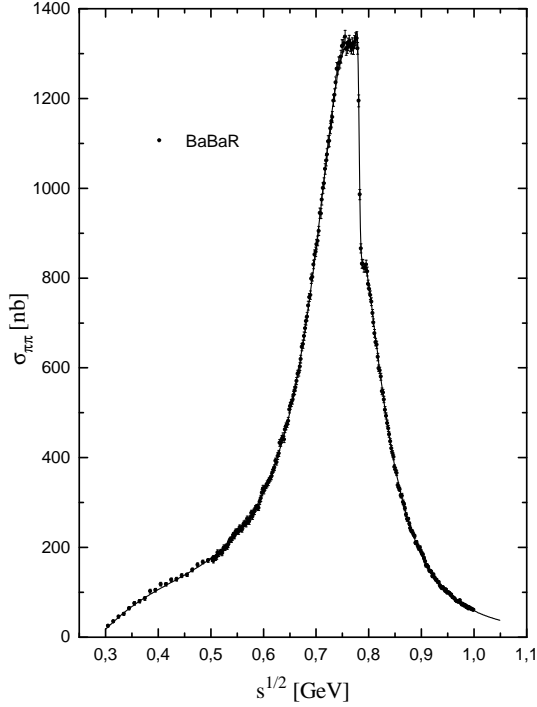


FIG. 5. The same as in Fig. 2, but evaluated with the parameters obtained from fitting the BaBar data [15] restricted to the energies $\sqrt{s} \leq 1$ GeV. Experimental points are from Ref. [15].

possible in closed form. In addition, the corresponding dispersion integrals diverge much more strongly than in the case of the $\pi^+\pi^-$ and $K\bar{K}$ intermediate states considered in the present work. In the meantime, the small values of $g_{\rho_{2,3}\pi\pi}$, in comparison with $g_{\rho_1\pi\pi}$, obtained in the present work upon neglecting the $\rho\pi\pi$, $\omega\pi$, etc., decay modes at $\sqrt{s} \leq 1$ GeV, agree with the earlier conclusions [7, 8] inferred from the analysis in which the above decay modes were included. Note also that a_{23} is compatible with zero.

V. DISCUSSION.

An important check of the expression for the pion form factor Eq. (3.1) and the consistency of the fits is the continuation to the spacelike region $t < 0$ accessible in the scattering processes. To this end, one should take the branch with $s < 0$ in $\Pi_{\pi,K}(s, m_V^2)$ [see Eqs. (2.8), (2.9), and (2.10)] and replace $s \rightarrow t$. Having in mind that the $\rho(770) - \omega(782)$ mixing in the region $t < 0$ is negligibly small one can calculate $F_\pi(t)$ in this region. The results are shown in Fig. 6, where the comparison with the NA7 data [21] is presented for all four fits considered in the present work. We emphasize that the data [21] are not included to the fits. Hence, a good agreement, demonstrated in Fig. 6, makes the evidence in favor of the validity of Eq. (3.1) for the pion form factor.

Using the resonance parameters of Table I, one can calculate, in particular, such important characteristics as the charged pion radius r_π , defined as the square root of the root-mean squared radius,

$$r_\pi = \sqrt{\langle r^2 \rangle},$$

of the spherical symmetric electric charge distribution

$$F_\pi(\mathbf{q}) = \int d^3r \rho(r) e^{i\mathbf{q}\cdot\mathbf{r}} \approx F_\pi(0) - \frac{\mathbf{q}^2}{6} \int \rho(r) r^2 d^3r = F_\pi(0) + \frac{t}{6} \langle r^2 \rangle, \quad (5.1)$$

where $t = -\mathbf{q}^2$. One gets

$$r_\pi = \sqrt{6 \frac{dF_\pi(t)}{dt} \Big|_{t \rightarrow 0}}. \quad (5.2)$$

Evaluating r_π with the parameters of Table I, one obtains the results presented in the first row of Table II. For comparison, the averaged value of the pion charge radius cited by the PDG [5] is $r_\pi = 0.672 \pm 0.008$ fm.

If one considers the single $\rho(770)$ resonance, then its inverse propagator near $s = m_{\rho_1}^2$ can be represented as

$$D_{\rho_1} = m_{\rho_1}^2 - s + (m_{\rho_1}^2 - s) \frac{d\text{Re}\Pi_{\rho_1\rho_1}(s)}{ds} \Big|_{s=m_{\rho_1}^2} -$$

TABLE II. The pion charge radius, r_π , Eq. (5.2), the renormalization constant, Z_ρ , Eq. (5.4), the "physical" partial widths (with the superscript phys), the bare ones (without the superscript), of the decay $\rho(770)$ and $\omega(782)$, evaluated with the resonance parameters of Table I.

parameter	SND	CMD-2	KLOE10	BaBaR
r_π [fm]	0.635 ± 0.054	0.646 ± 0.059	0.668 ± 0.039	0.668 ± 0.053
Z_ρ	0.9273 ± 0.0003	0.9277 ± 0.0002	0.9279 ± 0.0002	0.9277 ± 0.0001
$\Gamma_{\rho_1\pi\pi}(m_{\rho_1}^2)$ [MeV]	139.93 ± 0.29	139.54 ± 0.39	139.12 ± 0.29	139.34 ± 0.19
$\Gamma_{\rho_1\pi\pi}^{(\text{phys})}(m_{\rho_1}^2)$ [MeV]	150.90 ± 0.31	150.42 ± 0.42	149.92 ± 0.31	150.20 ± 0.20
$\Gamma_{\rho_1ee}(m_{\rho_1}^2)$ [keV]	6.56 ± 0.01	6.41 ± 0.01	6.29 ± 0.01	6.47 ± 0.01
$\Gamma_{\rho_1ee}^{(\text{phys})}(m_{\rho_1}^2)$ [keV]	7.07 ± 0.01	6.91 ± 0.01	6.78 ± 0.01	6.97 ± 0.01
$\Gamma_{\omega ee}(m_\omega^2)$ [keV]	0.59 ± 0.02	0.51 ± 0.03	0.52 ± 0.03	0.60 ± 0.02

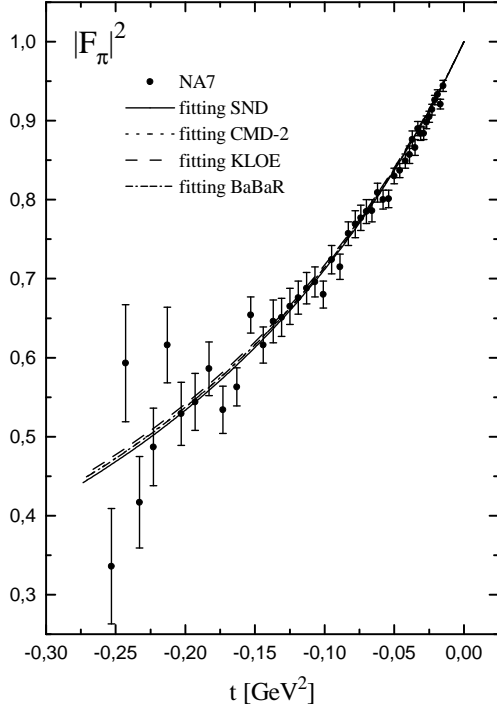


FIG. 6. The pion form factor squared in the spacelike region evaluated using the resonance parameters of Table I. The labels of the theoretical curves correspond to the columns of Table I. The experimental data NA7 are from Ref. [21].

$$i\sqrt{s}\Gamma_{\rho_1\pi\pi}(s). \quad (5.3)$$

The behavior of $\text{Re}\Pi_{\rho_1\rho_1}(s)$ is shown in Fig. 7. Comparing Eq. (5.3) with Eq. (1.1) one can see that one should make the renormalization

$$g_{\rho_1\pi\pi} \rightarrow Z_\rho^{-1/2} g_{\rho_1\pi\pi},$$

$$g_{\rho_1} \rightarrow Z_\rho^{1/2} g_{\rho_1},$$

where

$$Z_\rho = 1 + \frac{d\text{Re}\Pi_{\rho_1\rho_1}(s)}{ds} \Big|_{s=m_{\rho_1}^2}, \quad (5.4)$$

in order to reduce Eq. (5.3) to the conveniently used form with m_{ρ_1} being the physical mass of the resonance. This

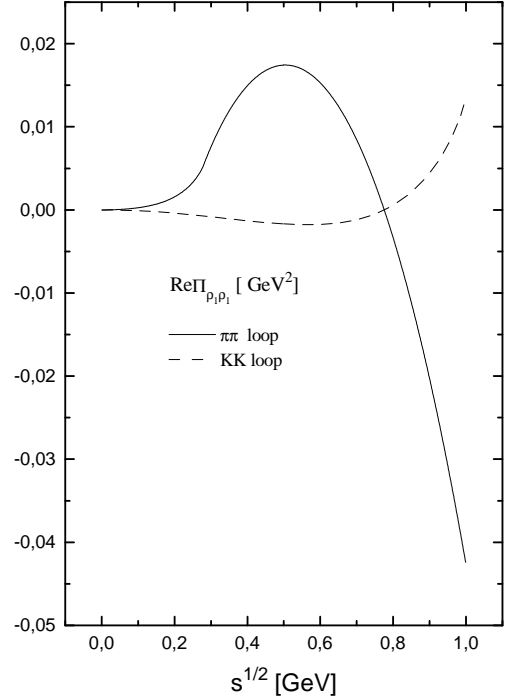


FIG. 7. The energy dependence of $\text{Re}\Pi_{\rho_1\rho_1}(s)$ for both $\pi^+\pi^-$ and $K\bar{K}$ loops.

results in the renormalization of the $\pi^+\pi^-$ and e^+e^- partial widths of the $\rho(770)$:

$$\begin{aligned} \Gamma_{\rho_1\pi\pi} &\rightarrow \Gamma_{\rho_1\pi\pi}^{(\text{phys})} = \frac{\Gamma_{\rho_1\pi\pi}}{Z_\rho}, \\ \Gamma_{\rho_1ee} &\rightarrow \Gamma_{\rho_1ee}^{(\text{phys})} = \frac{\Gamma_{\rho_1ee}}{Z_\rho}. \end{aligned} \quad (5.5)$$

The numerical values of the renormalization constant Z_ρ are given in Table II, side-by-side with the $\pi^+\pi^-$ and e^+e^- partial widths of the $\rho(770)$. One can see that Z_ρ brings the "bare" widths (without the superscript "phys") closer to the values $\Gamma_{\rho\pi\pi} = 149.1 \pm 0.8$ MeV and $\Gamma_{\rho ee} = 7.04 \pm 0.06$ keV cited in the Review of Particle Physics [5].

Another important characteristic of the low-energy hadronic physics is the phase shift δ_1^1 of $\pi\pi$ scattering in

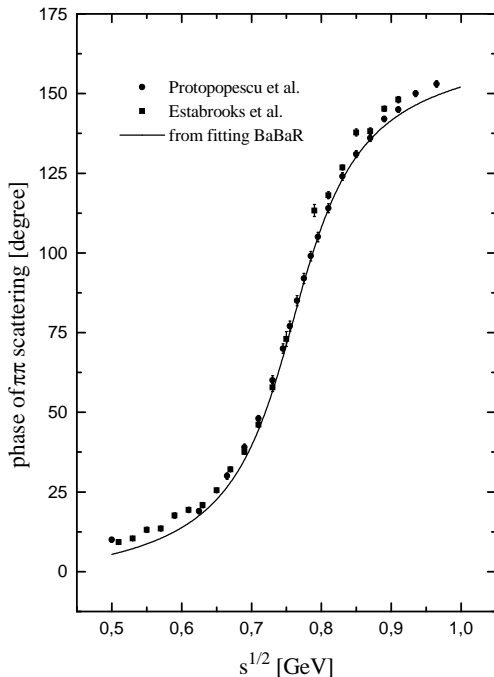


FIG. 8. The phase shift δ_1^1 of $\pi\pi$ scattering. The data are, respectively, Protopopescu et al. [26] and Estabrooks et al. [27]. The curves corresponding to the parameters obtained from fitting the SND, CMD-2, and KLOE data are not shown because they coincide with the curve evaluated using the parameters from the fit of the BaBar data, shown here.

the vector-isovector channel with the quantum numbers of $\rho(770)$. At energies below the $\omega\pi$ and $K\bar{K}$ production thresholds, δ_1^1 is given by the phase of the pion form factor

$$\delta_1^1 = \arctan \frac{\text{Im}F_\pi}{\text{Re}F_\pi}, \quad (5.6)$$

where F_π is given by Eq. (3.1) upon neglecting the contribution of $\rho\omega$ mixing $\propto \Pi_{\rho_1\omega}$. The plot of δ_1^1 , obtained using parameters extracted from fitting the low-energy portion of the BaBar data [15], is shown in Fig. 8, where the comparison with the data [26, 27] is presented. Note that the resonance parameters, extracted from three other sets of data [12–14], result in the curves for δ_1^1 coincident with that shown in Fig. 8. Having in mind that the data on the phase shift were not included in the fits, the agreement of the calculated δ_1^1 with the measured one is satisfactory.

VI. CONCLUSION

It is shown that the new formula for $F_\pi(s)$, Eq. (3.1), gives a good description of the latest experimental data [12–15] on the production of the $\pi^+\pi^-$ pair in e^+e^- annihilation at $\sqrt{s} < 1$ GeV. In this low-energy domain, one can restrict oneself by the contribution of the $\pi^+\pi^-$

and $K\bar{K}$ loops to both diagonal and nondiagonal polarization operators. In principle, other intermediate states could be taken into account, at least numerically. However, heavier isovector resonances $\rho(1450)$ and $\rho(1700)$ are known to have other decay modes besides $\pi^+\pi^-$ and $K\bar{K}$, such as $\omega\pi$, $a_1\pi$ etc. The treatment should include the energies $\sqrt{s} \leq 2$ GeV where the coupling constants with the above states could be determined. No data exist on these decay modes of the quality comparable with the $\pi^+\pi^-$ data [12–15]. Hence, at present, the restriction to the domain $\sqrt{s} < 1$ GeV and to the pseudoscalar loops seems justifiable.

ACKNOWLEDGMENTS

We are grateful to M. N. Achasov for numerous discussions which stimulated the present work.

Appendix A: The finite width and the resonance mixing

Some details necessary for taking into account the finite width effects and the resonance mixing are given in this Appendix. The meaning of the diagonal polarization operator $\Pi_{RR}(s)$ is that it modifies the inverse bare propagator of the resonance R with the mass m_R , $D_R^{(0)}(s) \equiv D_R^{(0)} = m_R^2 - s$, in the following way:

$$\begin{aligned} \frac{1}{D_R(s)} &= \frac{1}{D_R^{(0)}} + \frac{1}{D_R^{(0)}} \Pi_{RR}(s) \frac{1}{D_R^{(0)}} + \\ &\quad \frac{1}{D_R^{(0)}} \Pi_{RR}(s) \frac{1}{D_R^{(0)}} \Pi_{RR}(s) \frac{1}{D_R^{(0)}} + \dots = \\ &\quad \frac{1}{D_R^{(0)} - \Pi_{RR}(s)}. \end{aligned}$$

In particular, this formula takes into account the finite width effects

$$D_R(s) = m_R^2 - s - \text{Re}\Pi_{RR}(s) - i\sqrt{s}\Gamma_{R\pi\pi}(s). \quad (\text{A1})$$

In principle, the mixing of the isovector resonances $\rho(770)$, $\rho(1450)$, and $\rho(1700)$ can be strong, especially because of the common decay modes, for example, the $\pi^+\pi^-$ one. It can be taken into account in the field-theory-inspired approach based on summing to all orders of the loop corrections to the bare propagators of vector mesons [7, 8, 18, 20]. The term "bare" means that the propagators are not distorted by the mixing. The scheme can be demonstrated by taking the two-resonance mixing as an example [20]. It reduces in this case to the following replacements:

$$\begin{aligned} \frac{1}{D_R} &\rightarrow \frac{1}{D_R} + \frac{1}{D_R} \Pi_{RR'} \frac{1}{D_{R'}} \Pi_{RR'} \frac{1}{D_R} + \dots = \\ &\quad \frac{D_{R'}}{D_R D_{R'} - \Pi_{RR'}^2} \equiv (G^{-1})_{RR}, \end{aligned}$$

$$\begin{aligned} \frac{1}{D_{R'}} &\rightarrow \frac{1}{D_{R'}} + \frac{1}{D_{R'}} \Pi_{RR'} \frac{1}{D_R} \Pi_{RR'} \frac{1}{D_{R'}} + \dots = \\ &\frac{D_R}{D_R D_{R'} - \Pi_{RR'}^2} \equiv (G^{-1})_{R'R'}, \\ \frac{\Pi_{RR'}}{D_R D_{R'}} &\rightarrow \frac{\Pi_{RR'}}{D_R D_{R'}} + \frac{(\Pi_{RR'})^3}{(D_R D_{R'})^2} + \dots = \\ &\frac{\Pi_{RR'}}{D_R D_{R'} - \Pi_{RR'}^2} \equiv (G^{-1})_{RR'}. \end{aligned}$$

The matrix

$$G = \begin{pmatrix} D_R & -\Pi_{RR'} \\ -\Pi_{RR'} & D_{R'} \end{pmatrix}$$

is the matrix of inverse propagators in the two-resonance case. Let us take for a moment just this case, $R = \rho_1$ and $R' = \rho_2$, in order to clarify the effect of the mixing on the resonance position. Neglecting for a moment the $\rho\omega$ mixing which is taken into account below, one can write the pion form factor as

$$F_\pi = (g_{\gamma\rho_1}, g_{\gamma\rho_2}) \begin{pmatrix} D_{\rho_2} & \Pi_{\rho_1\rho_2} \\ \Pi_{\rho_1\rho_2} & D_{\rho_1} \end{pmatrix} \begin{pmatrix} g_{\rho_1\pi\pi} \\ g_{\rho_2\pi\pi} \end{pmatrix} \times \frac{1}{D_{\rho_1} D_{\rho_2} - \Pi_{\rho_1\rho_2}^2}. \quad (\text{A2})$$

In the vicinity of the ρ_1 resonance position, $s \rightarrow m_{\rho_1}^2$, Eq. (A2) can be represented in the form

$$F_\pi(s) \approx \frac{g_{\gamma\rho_1} g_{\rho_1\pi\pi}}{m_{\rho_1}^2 - s - \Pi_{\rho_1\rho_1}(s) - \frac{\Pi_{\rho_1\rho_2}^2(m_{\rho_1}^2)}{m_{\rho_2}^2 - m_{\rho_1}^2 - \Pi_{\rho_2\rho_2}(m_{\rho_1}^2)}}, \quad (\text{A3})$$

where, in accord with the adopted definition, $\text{Re}\Pi_{\rho_1\rho_1}(m_{\rho_1}^2) = 0$. One can see from Eq. (A3) that there is a shift in the ρ_1 resonance peak position due to the mixing of ρ_1 with the resonance ρ_2 :

$$\begin{aligned} \Delta m_{\rho_1}^2 &= -\text{Re} \frac{\Pi_{\rho_1\rho_2}^2(m_{\rho_1}^2)}{m_{\rho_2}^2 - m_{\rho_1}^2 - \Pi_{\rho_2\rho_2}(m_{\rho_1}^2)} \approx \\ &-\frac{\text{Re} [\Pi_{\rho_1\rho_2}^2(m_{\rho_1}^2)]}{m_{\rho_2}^2 - m_{\rho_1}^2}, \end{aligned} \quad (\text{A4})$$

where we neglect $\Pi_{\rho_2\rho_2}(m_{\rho_1}^2)$ in comparison with the mass difference squared $m_{\rho_2}^2 - m_{\rho_1}^2$. Indeed, using the plots in Fig. 7, the relation

$$\Pi_{\rho_2\rho_2} = \left(\frac{g_{\rho_2\pi\pi}}{g_{\rho_1\pi\pi}} \right)^2 \Pi_{\rho_1\rho_1},$$

Eq. (2.5), Eq. (2.7), and $g_{\rho_2\pi\pi} \approx 0.8$ (see Table I), one obtains the estimate

$$\frac{\Pi_{\rho_2\rho_2}(m_{\rho_1}^2)}{m_{\rho_2}^2 - m_{\rho_1}^2} \lesssim (0.2 + 1.5i) \times 10^{-3}.$$

In the case of the well-studied resonance $\rho_1 = \rho(770)$, it is natural to expect that the visible peak position with a good accuracy coincides with the bare mass m_{ρ_1} . This follows from the definition $\text{Re}\Pi_{\rho_1\rho_1}(m_{\rho_1}^2) = 0$ adopted in the present work. In order to preserve the above coincidence, the natural demand is to set $\text{Re}\Pi_{\rho_1\rho_2} = 0$. Since, in Eq. (A4), $\text{Re}\Pi_{\rho_1\rho_2}^2 = (\text{Re}\Pi_{\rho_1\rho_2})^2 - (\text{Im}\Pi_{\rho_1\rho_2})^2$, then, to be precise, some mass shift survives which is equal to

$$\Delta m_{\rho_1} \approx \frac{m_{\rho_1} \Gamma_{\rho_1\pi\pi}^2(m_{\rho_1}^2)}{2(m_{\rho_2}^2 - m_{\rho_1}^2)} \left(\frac{g_{\rho_2\pi\pi}}{g_{\rho_1\pi\pi}} \right)^2.$$

However, even in the worse case $g_{\rho_2\pi\pi} = 0.8$ (see Table I, where the magnitudes of the coupling constants extracted

from the specific fits are given), this shift is estimated at the level of 0.1 MeV. This estimate falls within the errors of m_{ρ_1} , quoted in Table I. Having in mind the three-resonance case, we set $\text{Re}\Pi_{\rho_1\rho_3} = 0$. Such a type of justification is not applicable for the poorly studied resonances $\rho_2 = \rho(1450)$ and $\rho_3 = \rho(1700)$; hence, the parameter a_{23} fixing $\text{Re}\Pi_{\rho_2\rho_3}$ remains free.

The generalization to the case of three (and any number of) resonances ρ_1, ρ_2 , and ρ_3 is straightforward. The matrix of inverse propagators is given by Eq. (3.4). The matrix of propagators is

$$G^{-1} = \frac{1}{\Delta} \begin{pmatrix} g_{11} & g_{12} & g_{13} \\ g_{12} & g_{22} & g_{23} \\ g_{13} & g_{23} & g_{33} \end{pmatrix},$$

where

$$\begin{aligned} g_{11} &= D_{\rho_2} D_{\rho_3} - \Pi_{\rho_2\rho_3}^2, \\ g_{22} &= D_{\rho_1} D_{\rho_3} - \Pi_{\rho_1\rho_3}^2, \\ g_{33} &= D_{\rho_1} D_{\rho_2} - \Pi_{\rho_1\rho_2}^2, \\ g_{12} &= D_{\rho_3} \Pi_{\rho_1\rho_2} + \Pi_{\rho_1\rho_3} \Pi_{\rho_2\rho_3}, \\ g_{13} &= D_{\rho_2} \Pi_{\rho_1\rho_3} + \Pi_{\rho_1\rho_2} \Pi_{\rho_2\rho_3}, \\ g_{23} &= D_{\rho_1} \Pi_{\rho_2\rho_3} + \Pi_{\rho_1\rho_3} \Pi_{\rho_2\rho_1}, \\ \Delta &\equiv \det G = D_{\rho_1} D_{\rho_2} D_{\rho_3} - 2\Pi_{\rho_1\rho_2} \Pi_{\rho_1\rho_3} \Pi_{\rho_2\rho_3} - \\ &D_{\rho_1} \Pi_{\rho_2\rho_3}^2 - D_{\rho_2} \Pi_{\rho_1\rho_3}^2 - D_{\rho_3} \Pi_{\rho_1\rho_2}^2. \end{aligned} \quad (\text{A5})$$

Note that, deep in the spacelike domain, the quantity $1/\Delta$ and, as a consequence, the pion form factor have a pole at $\sqrt{-t} = 87, 82, 97$, and 95 GeV, when evaluated with the resonance parameters obtained from the fit of, respectively, SND [12], CMD-2 [13], KLOE [14], and BaBar [15] data. This pole is the analog of the famous Landau pole.

In addition to the strong mixing between the isovector resonances, one should include also the isovector-isoscalar

$\rho_i - \omega(782)$ mixing arising due to small G-parity breaking. Then, the matrix of inverse propagators can be written in the form

$$G_{\text{tot}} = \begin{pmatrix} D_{\rho_1} & -\Pi_{\rho_1\rho_2} & -\Pi_{\rho_1\rho_3} & -\Pi_{\rho_1\omega} \\ -\Pi_{\rho_1\rho_2} & D_{\rho_2} & -\Pi_{\rho_2\rho_3} & -\Pi_{\rho_2\omega} \\ -\Pi_{\rho_1\rho_3} & -\Pi_{\rho_2\rho_3} & D_{\rho_3} & -\Pi_{\rho_3\omega} \\ -\Pi_{\rho_1\omega} & -\Pi_{\rho_2\omega} & -\Pi_{\rho_3\omega} & D_{\omega} \end{pmatrix} \quad (\text{A6})$$

$$\begin{aligned} g_{\omega\pi\pi}^{(\text{eff})} &\approx g_{\omega\pi\pi} - \frac{(\text{Re}\Pi_{\rho_1\omega} + i\text{Im}\Pi_{\rho_1\omega})g_{\rho_1\pi\pi}}{m_{\omega}^2 - m_{\rho_1}^2 - i\sqrt{s}(\Gamma_{\omega} - \Gamma_{\rho_1\pi\pi})} = \frac{1}{m_{\omega}^2 - m_{\rho_1}^2 - i\sqrt{s}(\Gamma_{\omega} - \Gamma_{\rho_1\pi\pi})} \{g_{\omega\pi\pi} [m_{\omega}^2 - m_{\rho_1}^2 - \\ &i\sqrt{s}(\Gamma_{\omega} - \Gamma_{\rho_1\pi\pi})] - g_{\rho_1\pi\pi} \left[\text{Re}\Pi_{\rho_1\omega} + i \left(\text{Im}\tilde{\Pi}_{\rho_1\omega} + \sqrt{s} \frac{g_{\omega\pi\pi}}{g_{\rho_1\pi\pi}} \Gamma_{\rho_1\pi\pi} \right) \right] \} \approx \\ & - \frac{(\text{Re}\Pi_{\rho_1\omega} + i\text{Im}\tilde{\Pi}_{\rho_1\omega})g_{\rho_1\pi\pi}}{m_{\omega}^2 - m_{\rho_1}^2 - i\sqrt{s}(\Gamma_{\omega} - \Gamma_{\rho_1\pi\pi})}, \end{aligned} \quad (\text{A8})$$

where $\text{Im}\tilde{\Pi}_{\rho_1\omega}$ differs from $\text{Im}\Pi_{\rho_1\omega}$ by the absence of the term $\propto g_{\omega\pi\pi}$. Hence, one can safely neglect the coupling constant $g_{\omega\pi\pi}$. This circumstance was not properly accounted for in our earlier work, Ref. [7]. The isovector-isoscalar type of weak mixing is essential only for the $\rho(770) - \omega(782)$ system because it is enhanced due to the small mass difference of these resonances. See Eq. (A8). As for other isovector-isoscalar mixings $\rho(1450) - \omega(782)$ and $\rho(1700) - \omega(782)$, there is no enhancement, due to the mass proximity, and one can neglect $\Pi_{\rho_{2,3}\omega}$. Taking the latter assumption into account and allowing for the $\rho_1\omega$ mixing to first order, one can approximate the propagator matrix G^{-1} in Eq. (A7) by the expression

$$G_{\text{tot}}^{-1} \approx \frac{1}{\Delta} \begin{pmatrix} g_{11} & g_{12} & g_{13} & \frac{g_{11}\Pi_{\rho_1\omega}}{D_{\omega}} \\ g_{12} & g_{22} & g_{23} & \frac{g_{12}\Pi_{\rho_1\omega}}{D_{\omega}} \\ g_{13} & g_{23} & g_{33} & \frac{g_{13}\Pi_{\rho_1\omega}}{D_{\omega}} \\ \frac{g_{11}\Pi_{\rho_1\omega}}{D_{\omega}} & \frac{g_{12}\Pi_{\rho_1\omega}}{D_{\omega}} & \frac{g_{13}\Pi_{\rho_1\omega}}{D_{\omega}} & \frac{\Delta}{D_{\omega}} \end{pmatrix},$$

In this case, the pion form factor is written as follows:

$$F_{\pi}(s) = (g_{\gamma\rho_1}, g_{\gamma\rho_2}, g_{\gamma\rho_3}, g_{\gamma\omega}) G^{-1} \begin{pmatrix} g_{\rho_1\pi\pi} \\ g_{\rho_2\pi\pi} \\ g_{\rho_3\pi\pi} \\ g_{\omega\pi\pi} \end{pmatrix}, \quad (\text{A7})$$

The coupling constant $g_{\omega\pi\pi}$ describes the direct $\omega \rightarrow \pi^+\pi^-$ transition arising due to the violation of G-parity conservation side-by-side with the mixing mechanism. However, it is known [28] that, since the $\pi^+\pi^-$ channel dominates the ρ_1 decay width, $g_{\omega\pi\pi}$ is almost canceled in the effective $\omega \rightarrow \pi^+\pi^-$ transition amplitude due to the compensation among imaginary parts of $\Pi_{\rho_1\omega}$ and the inverse ρ_1 propagator. Indeed, allowing for both the mixing and direct transition, one can write the effective $\omega\pi\pi$ coupling constant in the form

where the g_{ij} and Δ are given by Eq. (A5). The final approximate expression for the pion form factor $F_{\pi} \equiv F_{\pi}(s)$ given by Eq. (3.1) is obtained by inserting this approximate expression to Eq. (A7) and by neglecting the coupling constant of the direct decay $g_{\omega\pi\pi}$.

- [1] J. J. Sakurai. Ann. Phys. (N.Y) **11**, 1 (1960).
- [2] M. Gell-Mann and F. Zachariasen. Phys. Rev. **124**, 953 (1961).
- [3] N. M. Kroll, T. D. Lee, and B. Zumino. Phys. Rev. **157**, 1376 (1967).
- [4] J. H. Lowenstein and B. Schroer. Phys. Rev. D **6**, 1553 (1972).
- [5] K. Nakamura, *et al.* (Particle Data Group), Journal of Physics **G37**, 075021 (2010).

- [6] G. J. Gounaris and J. J. Sakurai. Phys.Rev.Lett. **21**, 244 (1968).
- [7] N. N. Achasov and A. A. Kozhevnikov. Phys.Rev.D **55**, 2663 (1997) [arXiv:hep-ph/9609216v1].
- [8] N. N. Achasov and A. A. Kozhevnikov. Yad.Fiz. **60**, 1131 (1997); Phys.Atom.Nucl. **60**, 1011-1019 (1997) [arXiv:hep-ph/9607398].
- [9] C. Gale and J. Kapusta. Nucl. Phys. B **257**, 65 (1991).
- [10] C. A. Dominguez, J. I. Jottar, M. Loewe, and B. Willers.

- Phys. Rev. D**76**, 095002 (2007).
- [11] C. A. Dominguez, M. Loewe, and B. Willers. Phys. Rev. D**78**, 057901 (2008).
 - [12] M. N. Achasov, *et al.*. J.Exp.Theor.Phys. **101**, 1053 (2005); Zh.Eksp.Teor.Fiz. **101**, 1201 (2005) [arXiv:hep-ex/0506076v1].
 - [13] CMD-2 Collaboration: R. R. Akhmetshin, *et al.* Phys.Lett.B**648**, 28 (2007) [arXiv:hep-ex/0610021v3].
 - [14] KLOE Collaboration, F. Ambrosino, *et al.* "Measurement of $\sigma(e^+e^- \rightarrow \pi^+\pi^-)$ from threshold to 0.85 GeV² using Initial State Radiation with the KLOE detector". [arXiv:1006.5313v1].
 - [15] The BABAR Collaboration: B. Aubert, *et al.* Phys.Rev.Lett.**103**, 231801 (2009) [arXiv:0908.3589v1].
 - [16] M. Gell-Mann. *The Eightfold Way: A Theory of strong interaction symmetry*. CalTech preprint CTSL-20, TID-12608 (1961).
 - [17] Y. Ne'eman. Nucl. Phys. **26**, 222 (1961).
 - [18] N. N. Achasov, S. A. Devyanin, and G. N. Shestakov. Usp. Fiz. Nauk **142**, 361 (1984); Sov.Phys.Usp.**27**, 161 (1984).
 - [19] N. N. Achasov, S. A. Devyanin, and G. N. Shestakov. Z.Phys.C**22**, 53 (1984).
 - [20] N. N. Achasov and A. A. Kozhevnikov. Talk at IX International Conference on Hadron Spectroscopy, 25 August-1 September, 2001, IHEP, Protvino, Russia. AIP Conf.Proc. **619**, 687 (2002). [arXiv:hep-ph/0110039v1].
 - [21] S. R. Amendolia, *et al.* Nucl.Phys.B**277**, 168 (1986).
 - [22] J. S. Schwinger. *Particles, Sources and Fields. Volume II*, (Addison-Wesley Publishing Company, Reading, MA, 1973).
 - [23] M. Deers and K. Hikasa. Phys. Lett. B**252**, 127 (1990).
 - [24] K. Melnikov. Int. Journ. Mod. Phys. A**16**, 4591 (2001).
 - [25] A. Hoefer, J. Gluza, and F. Jegerlehner. Eur. Phys. Journ. C**24**, 51 (2002).
 - [26] S. D. Protopopescu, *et al.* Phys. Rev. D**7**, 1279 (1973).
 - [27] P. Estabrooks and A. D. Martin. Nucl. Phys. B**79**, 301 (1974)
 - [28] M. Gourdin, F. M. Renard, and L. Stodolsky. Phys.Lett. **B30**, 347 (1969).